J. Exp. Biol. (1970), 53, 445–464
With 1 plate and 11 text-figures
Printed in Great Britain

BENDING MOMENTS IN FREE-SWIMMING FLAGELLA*

By C. J. BROKAW
Division of Biology, California Institute of Technology
Pasadena, California 91109

(*Received* 18 *May* 1970)

INTRODUCTION

The bending of a flagellum, such as the flagellum which forms the tail of a sea-urchin spermatozoon, is the result of active mechanochemical processes occurring within the flagellum itself, which cause it to bend actively throughout its length (Gray, 1955; Machin, 1958). To understand how flagella operate, we must understand not only the mechanisms which generate bending, but also the control mechanisms which initiate and coordinate the active bending of different parts of the flagellum in order to generate smoothly propagated bending waves which will efficiently propel a cell.

Spermatozoa, such as sea-urchin spermatozoa, which propagate nearly planar waves of bending along their flagella, can be readily photographed to reveal the shape of the flagellum during active movement. Such photographs indicate that the bending waves are ordinarily composed of bent regions, in which the flagellum is bent into a circular arc, separated by shorter regions in which the flagellum is approximately straight (Brokaw & Wright, 1963; Brokaw, 1965). As bent regions move along a flagellum, bending and unbending of the flagellum are therefore occurring only in rather short transition zones between the bent and straight regions. These transition zones, which I will refer to as bending or unbending points, move relatively uniformly along the flagellum to produce propagated bending waves. After sudden breakage of the flagellum by a laser microbeam, bent regions already established in the distal fragment of the flagellum continue to propagate to the end of the flagellum, although no new bent regions are formed (Goldstein, 1969). Therefore, either the bent region as a whole, or the bending and unbending points at its ends, appear to be autonomous, self-propagating, events. Other aspects of this picture of flagellar bending have been discussed elsewhere (Brokaw, 1966*a*, 1968). The present paper has been motivated by the following question: Is the propagation velocity of a bent region, or of its bending and unbending points, determined by the resistance which these events encounter as they move from point to point along the flagellum? Since the propagation velocity can vary, for example, when the viscosity of the medium is altered (cf. Brokaw, 1966*b*), some mechanism must exist to control this potentially variable velocity, in order to produce a particular bending wave pattern.

The resistance to bending (or to unbending) can be expressed as a bending moment which will be a function of time and position along the length of the flagellum. This

* This work has been supported in part by a grant from the United States Public Health Service (GM 14613).

moment will be the sum of a non-conservative moment resulting from forces acting on the flagellum as it moves against the viscous resistance of the surrounding medium, a conservative moment resulting from the internal elasticity of the flagellum, and, possibly, non-conservative moments originating within the flagellum. Only the moment resulting from external viscous forces is accessible to determination in moving flagella, although by making various assumptions, estimates of internal elasticity can be obtained subsequently. Such estimates have been made in a number of studies (Gray, 1955; Machin, 1958; Rikmenspoel, 1966; Brokaw, 1966*b*).

A calculation of the bending moment resulting from viscous forces on a moving flagellum was described in an earlier paper (Brokaw, 1965). This calculation involved assumptions which were only appropriate for a segment of an infinitely long flagellum. It gave no indication of the variation in moment which must occur near the ends of a finite flagellum. An improved method for calculating bending moments resulting from viscous forces on a finite flagellum has now been developed which makes use of numerical integration by high-speed digital computer. This method can handle any form of planar bending movement, including asymmetrical bending patterns such as those commonly found on cilia, and waves with parameters which vary with time or position along the flagellum. In this paper the method is used to analyse data from some new photographs of the movement of sea-urchin sperm flagella. The mathematical methods used for computing bending moments are described in an Appendix. With the exception of the first paragraph of the Appendix, which outlines the fundamental assumptions of the method, knowledge of these mathematical details should not be necessary for interpretation of the results of the paper.

DATA AND METHODS OF ANALYSIS

As described in the Appendix, the bending moments resulting from viscous forces on a moving flagellum can be calculated from data describing the bending behaviour of the flagellum. This data must include the position and propagation velocity of each bending and unbending point, and either the curvature and its rate of change with time, or the angle and its rate of change, of each bent region.

The photographs in Plate 1 record the movement of headless sperm flagella from the sea urchin *Lytechinus pictus*. These photographs were obtained by the same methods used in earlier work (Brokaw, 1965), except that the use of an improved stroboscopic illuminator (model 135 N, Chadwick-Helmuth Co., Monrovia, Calif.) has enabled me to record a greater number of positions of a flagellum on a single photograph. These photographs provide information about the behaviour of bends near the base of the flagellum which has not been available previously. Using several enlarged copies of these photographs, each image of the flagellum was analysed in the following manner.

First, a set of circles inscribed on a sheet of transparent plastic was used to locate the centre of curvature of each bent region of the flagellum. Using these centres, circles were drawn passing along the midline of the image of the flagellum in the bent regions; the radii of these circles were measured to obtain the curvature of the flagellum in each bent region. Secondly, lines were drawn tangent to adjacent circles, to locate the straight regions of the flagellum. The angles between the lines forming the straight regions were measured with a protractor in order to determine the total angle of bend

in each bent region. Thirdly, lines were drawn perpendicular to the straight regions, passing through the centres of curvature of the bent regions. The intersections between these perpendiculars and the lines forming the straight regions located the bending and unbending points. The distance of each of these points from the basal end of the flagellum was determined by measuring the lengths of the straight regions, and by calculating the arc lengths in the bent regions from the angle of bend and the curvature. Most of the images in the photographs I have selected for detailed study could be accurately matched by this procedure.

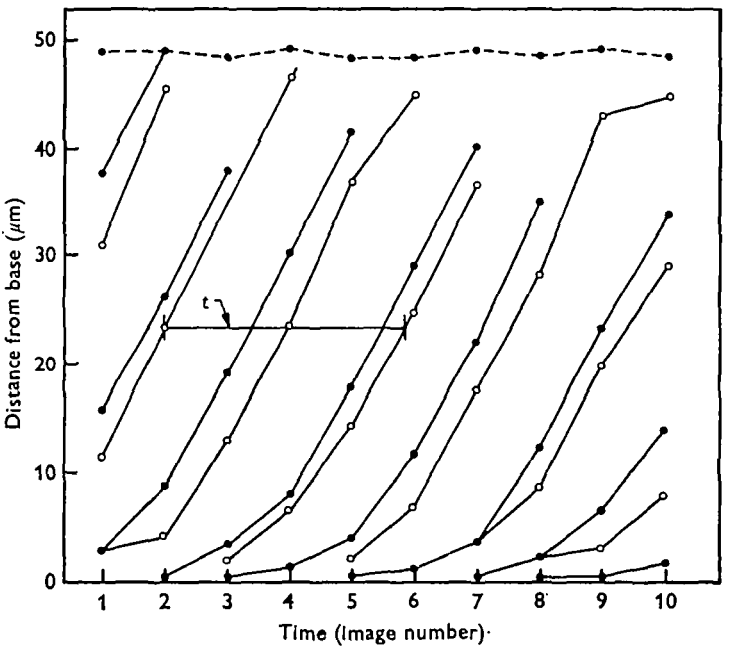

Text-fig. 1. Locations of bending and unbending points measured from Pl. 1, fig. 1. ○, Bending points; ●, unbending points. The points at the upper edge of the figure are measurements of the total length of the flagellum. The line marked *t* is an example of the measurements made to estimate the duration of the beat cycle.

The results of measuring Pl. 1, fig. 1, are shown in Text-figs. 1–3. In Text-fig. 1 the positions of each bending and unbending point, measured from the base of the flagellum, have been plotted as functions of time (determined by the image sequence). The lines connect successive positions of a particular bending or unbending point. The variation in the measured positions of the distal end of the flagellum gives an indication of the magnitude of the errors involved in taking measurements from these photographs.

Inspection of Text-fig. 1 indicates that the bending and unbending points propagate slowly near the base of the flagellum, but accelerate to a reasonably constant propagation velocity in the distal three-quarters of the flagellum.

The time period corresponding to one full cycle of bending in the distal part of the flagellum was obtained in the following manner. Distance parallel to the time axis in Text-fig. 1 was measured from each plotted point to the connecting line corresponding

to the next repetition of that phase point. The line marked t in Text-fig. 1 is an example of such a measurement. The average of all possible measurements of this type was found to be 3·65 flash intervals. The points in Text-fig. 1 were then replotted in Text-fig. 2, using lateral shifts of an integral multiple of 3·65 flash intervals, where necessary, to put all the positions of each type (+ or −) of bending or unbending point in one sequence. The resulting sequences show more irregularity than is evident from the

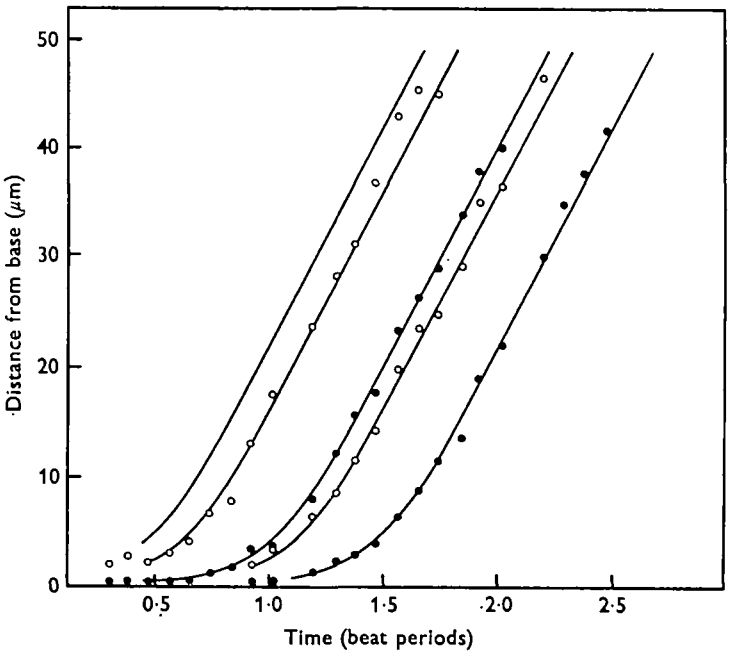

Text-fig. 2. Data from Text-fig. 1, after time-shifting of points to produce a single sequence of locations for each type of bending point. ○, Bending points; ●, unbending points. The origin of the time scale would correspond to the point of zero propagation velocity for the leading bending point, according to the $V_s = t^2$ equation used to derive the curves in the basal region of the flagellum. The same time scale has been used in Text-figs. 3 and 6.

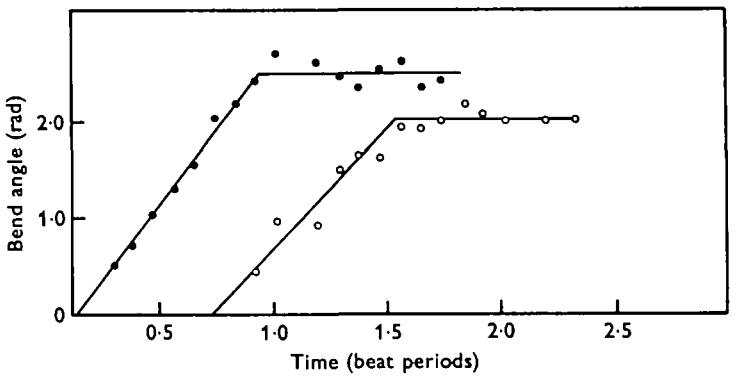

Text-fig. 3. Measured values of the total angle of bend in bent regions of the flagellum in Pl. 1, fig. 1. The angles for the two bends should actually have opposite signs, but the values are plotted as shown for compactness. The times correspond to those in Text-fig. 2.

lines in Text-fig. 1; this represents noise introduced by variations in the behaviour of the flagellum during different beat cycles. The set of parallel straight lines shown in Text-fig. 2 was fitted by eye to the points in the distal portion of the flagellum. With one possible exception the deviations from these lines appear to be in the nature of random noise, rather than repeated non-uniformities in the propagation velocity of bending and unbending points. However, a larger sequence of data points would be required to establish this conclusion definitely.

The acceleration of propagation of bending and unbending points near the base of

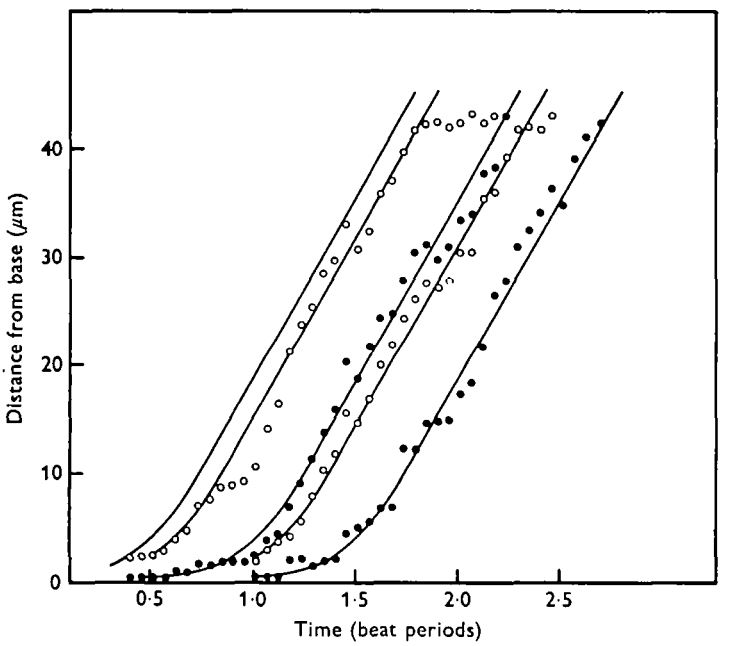

Text-fig. 4. Locations of bending and unbending points measured from Pl. 1, fig. 2. The beginning of the continous sequence of positions in the photograph corresponds to times of 0, 1·0, 2·0 cycles, etc.; in other respects the data are presented just as in Text-fig. 2.

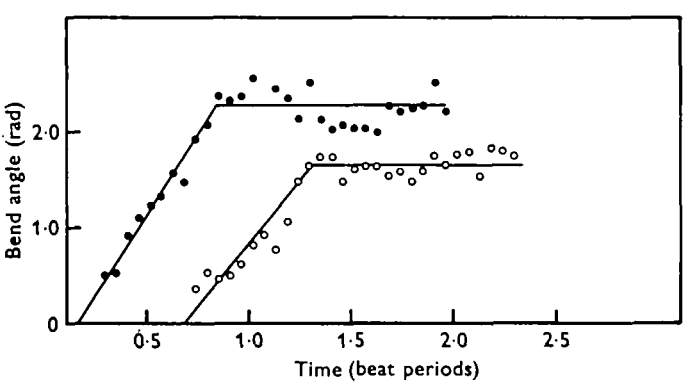

Text-fig. 5. Measured values of the total angle of bend in bent regions of the flagellum in Pl. 1, fig. 2, plotted as in Text-fig. 3. The time scale corresponds to that in Text-figs. 4 and 8.

the flagellum appears to follow a reasonably consistent pattern. For convenience in obtaining propagation velocities for input to the computer calculations, I have assumed that the propagation velocity increases with the square of time, until it reaches the constant value characteristic of the distal part of the flagellum. The sequence of positions generated by this assumption is indicated by the lines drawn in Text-fig. 2. These lines correspond to the input given to the computer about the behaviour of this flagellum. Although it would be possible to use the actual measured positions of bending and unbending points on the flagellum for input to the computer, the velocities of these points are also needed. Without having more closely spaced photographs, these velocities can only be obtained by making some assumptions about the uniformity of the movement, as incorporated into the lines drawn in Text-fig. 2.

The measured angles of the positive and negative bent regions have been plotted in Text-fig. 3 as a function of time, using the same time-shifting procedures as used to obtain Text-fig. 2. The angles increase gradually over slightly more than one half-cycle and then level off to an approximately constant value, so that there is little overlap between the periods of increase in angle of the positive and negative bends. As a consequence, the angular orientation of the basal end of the flagellum does not remain constant with respect to the distal portion of the flagellum, as appears to be the case in thiourea-inhibited spermatozoa (Brokaw, 1965). The linear functions indicated by the lines drawn in Text-fig. 3 have been used for computing the bending moments for this flagellum.

Given parameters for the lines drawn in Text-figs. 2 and 3, the data required for computation of bending moments can be calculated for any time in the bending cycle. Computations on this flagellum were performed at 24 evenly spaced times in the bending cycle.

Results of analysis of another flagellum, shown in Pl. 1, fig. 2, are presented by the graphs in Text-figs. 4 and 5. In this case the flash frequency was just slightly below the frequency of beat, and the 18 images appear to cover almost exactly one cycle of bending. However, the record is noisier; possibly because it covers a larger number of beat cycles than the one in Pl. 1, fig. 1. The lines used to obtain data for computation were obtained by the same procedures as used for the previous flagellum.

RESULTS OF BENDING-MOMENT COMPUTATION

A check on the validity of the computational methods can be carried out by comparing measured values for the average angular velocity and forward velocity of the flagellum in Pl. 1, fig. 2, with computed velocities obtained as part of the computation of bending moments. For this purpose the computation was carried out using several values for C_N/C_L, the ratio of normal and tangential drag coefficients. This flagellum rotated through an angle of about 198° in 17·95 beats, for an average angular velocity of 0·193 radians/beat. The computation gave values for W, the angular velocity of the basal end of the flagellum, at 18 times through the beat cycle. By integrating W over the beat cycle after subtracting the portion of W resulting from bending of the flagellum, agreement with the observed angular velocity was obtained for a value of C_N/C_L close to 1·8. A similar comparison of the path-length of this flagellum with the computed linear velocities of the basal end of the flagellum (V_x and V_y) gave best

agreement for a value of C_N/C_L close to 1·9. The second estimate is probably less precise.

C_N/C_L is expected to have a limiting value of 2·0 for an infinitesimally thin filament, and a somewhat lower value for a real filament. Equations given by Burgers (1938) and by Hancock (1953) suggest that C_N/C_L should have a value of about 1·7 for a filament having the dimensions of these flagella.

Considering the variability of the movement of this flagellum, and the approximation involved in extracting data from the photograph, the agreement between the two estimates of C_N/C_L and with theoretical values is satisfactory. This agreement suggests that the hydrodynamic assumptions on which the computational method is based are reasonably valid, and that no major errors have been made in developing the method.

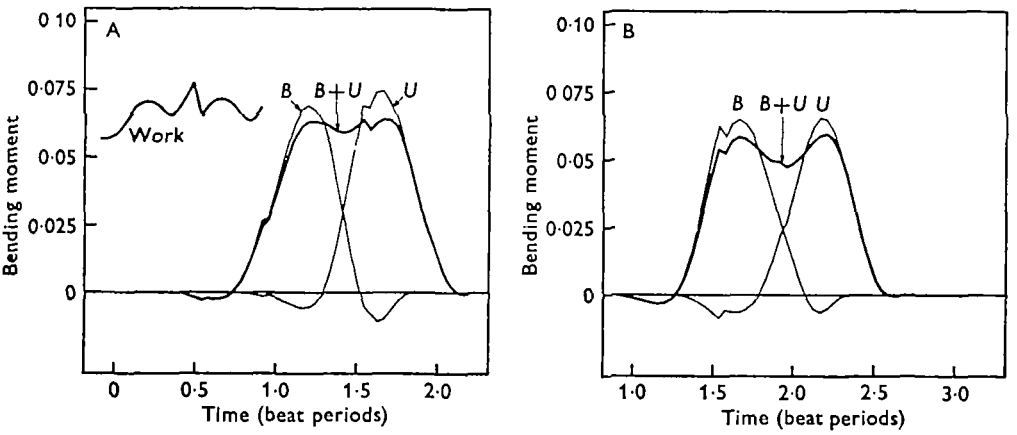

Text-fig. 6. Bending-moment curves computed for the flagellum in Pl. 1, fig. 1, by using data represented by the lines in Text-figs. 2 and 3. Text-fig. 6 A shows the curves for the bending and unbending points of the bend which reaches the larger angle of bending; B shows curves for the smaller bend. Other details are explained in the text.

A more thorough test of the hydrodynamic assumptions might be made by analysing a large number of photographs in a similar fashion. For further computations in this paper a value of $C_N/C_L = 1{\cdot}8$ has been used.

The results of the bending-moment computations, plotted in Text-figs. 6–9, are given in terms of a non-dimensional factor which depends on the shape of the bending wave pattern. This factor must be multiplied by $C_L f L^3$ to obtain actual values of bending moments, where f is the frequency of beat, and L is the wavelength measured along the flagellum, or $1/f$ times the value of the propagation velocity in the distal portion of the flagellum.

Text-fig. 6 presents bending-moment curves computed using the data obtained from Pl. 1, fig. 1. Three moment curves are shown in each half of this figure. Curve B gives values of the bending moment at a particular bending point as a function of time, from the time the bending point appears near the base of the flagellum until it reaches the distal end of the flagellum. Curve U gives values for the following unbending point, at corresponding times. All the curves have been plotted so that positive moments indicate a moment which opposes the bending at a bending point or the unbending

at an unbending point. Curve $B+U$ gives the value of the sum of the moments resisting bending and unbending at the ends of a complete bend at any given time.

Since the bending pattern of this flagellum is asymmetrical, different moment curves are obtained for the bends of positive and negative direction. Text-fig. 6A gives values of the moments for the bends of larger angle and Text-fig. 6B gives values for the bends of smaller angle. In Text-fig. 7A moments are shown for a symmetrical bending pattern derived from this flagellum by using mean values for the angles, etc., of the positive and negative bends. In Text-fig. 7B moments are shown for a symmetrical, uniform, bending pattern derived from this flagellum,

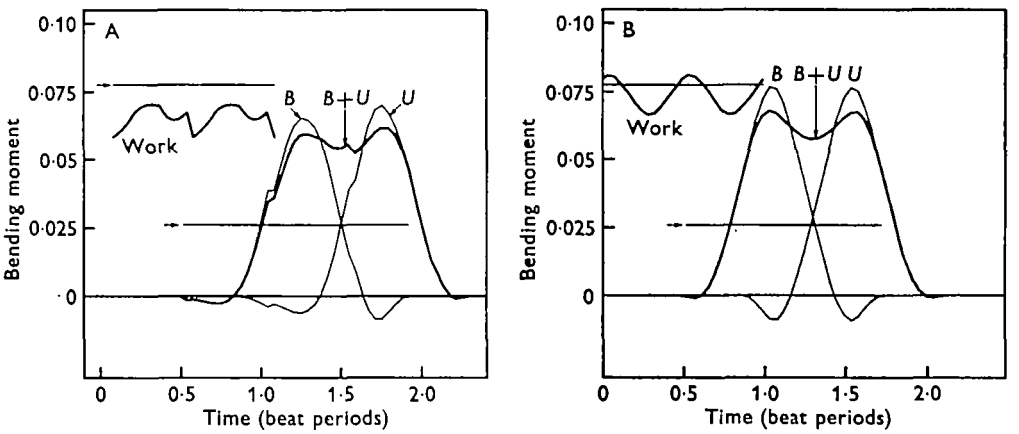

Text-fig. 7. Bending-moment curves computed for modified forms of flagellar movement derived from the data for the flagellum in Pl. 1, fig. 1. A applies to a symmetrical modification of the bending waves and B applies to a symmetrical, uniform, modification with no change in the curvature or propagation velocity of the bends near the base of the flagellum. The horizontal lines give the average values of moment and power output calculated by earlier, approximate methods.

having a constant propagation velocity for all bending points and a constant radius of curvature for all the bent regions; these values are obtained from the distal portion of the flagellum. This situation should most closely resemble that treated in previous work (Brokaw, 1965).

Values of the power output of the flagellum (labelled 'work') are also shown as a function of time in Text-figs. 6 and 7. These values are also given as dimensionless quantities, and must be multiplied by $10\ C_L f^2 L^3$ to obtain actual values for the power output. The power outputs shown in Text-figs. 6A and 7A include not only the work done at the bending and unbending points as they move along the flagellum, but also the work done in changing the curvature of bends in the bend-initiating region of the flagellum. The latter portion represents about 5% of the total work. The values for power may be about 5% too low, since the 'negative work' done in regions of negative moment is subtracted from the total.

Values for bending moment and power calculated by the earlier equations (Brokaw, 1965) are also indicated in Text-fig. 7 (horizontal lines marked by arrows). These equations give reasonably accurate estimates of the average values of bending moment and power output.

The curves in Text-figs. 6A, B and 7A contain discontinuities at the times at which the bend angles reach their final values and stop increasing linearly (see Text-fig. 3). This discontinuity in the rate of increase in bend angles may not be a real feature of the generation of bends in flagella, but there is not sufficient data from these photographs to settle this point.

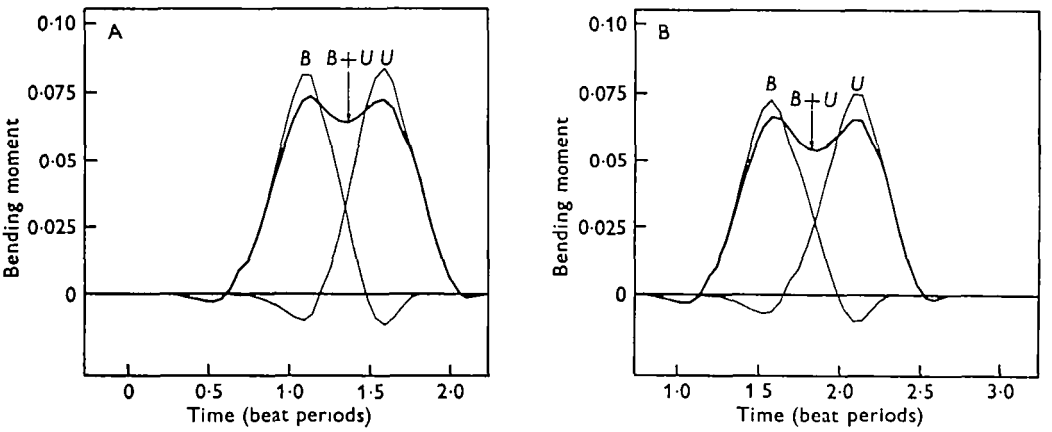

Text-fig. 8. Bending-moment curves computed for the flagellum in Pl. 1, fig. 2, by using data represented by the lines in Text-figs. 4 and 5. A and B are for the larger and smaller bends respectively, as in Text-fig. 6.

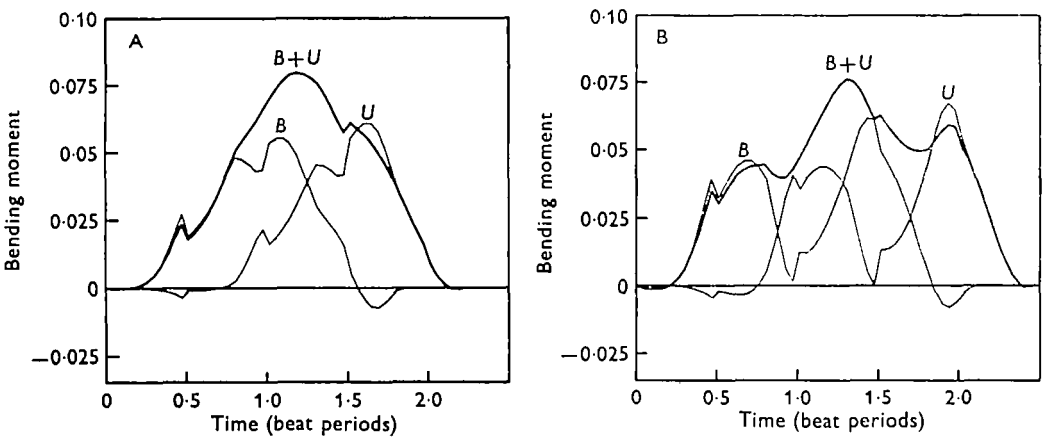

Text-fig. 9. Bending moment curves computed for modified forms of flagellar movement derived from the data for the flagellum in Pl. 1, fig. 1. In these cases, the movement is symmetrical, as in Text-fig. 7A, but the length of the flagellum has been increased from its original value of $1{\cdot}23L$ to values of $1{\cdot}75L$ in A and $2{\cdot}0L$ in B. (L is the wavelength, measured on the flagellum, of the bending waves on the distal part of the flagellum.)

Results of computations for the flagellum in Pl. 1, fig. 2, are presented in Text-fig. 8. This flagellum has wave parameters which are closer to the normal wave parameters for *Lytechinus* spermatozoa. The distributions of moments in the two cases examined here (Text-figs. 6, 8) are very similar.

The general form of the bending-moment curves in these figures is not greatly influenced by details of the parameters of the bending waves, the manner of initiation

of bends near the base of the flagellum, or the asymmetry of the bending wave pattern. Other calculations show, however, that the ratio (S/L) of the total length of the flagellum to the wavelength of the bending waves does influence the form of the bending-moment curves. Examples are shown in Text-fig. 9, using data from the symmetrical flagellum of Text-fig. 7A, except for changes in the value of S/L (S/L = 1·23 for the flagellum of Pl. 1, fig. 1, and S/L = 1·36 for the flagellum of Pl. 1, fig. 2). Moments calculated for S/L = 1·5 are not very different in form from those at the lower values of S/L in Text-figs. 6–8, but significantly different moment curves are obtained for values of S/L of 1·75 and 2·0. Bending patterns with values of S/L in this range can be produced by sea-urchin sperm flagella when the viscosity of the medium is increased (Brokaw, 1966*b*) and are normal for the movement of the posterior flagellum of the dinoflagellate, *Ceratium* (Brokaw & Wright, 1963).

Moments have also been calculated using data for an intact spermatozoon. The presence of the head causes only minor changes in the distribution of bending moments.

DISCUSSION

These calculations of the bending moments which result from the viscous resistance of the medium through which a flagellum is moving indicate that the viscous resistance encountered by a bending or unbending point as it moves along a flagellum varies significantly from one part of the flagellum to another. The bending moment is zero at each end of a headless flagellum. Near each end of the flagellum there is often a region where the resisting moment has negative values, meaning that bending and/or unbending in these regions could be driven indirectly by bending and unbending occurring in other parts of the flagellum. The resisting moments rise to peak values of about 2·5 times their average value near the middle of the flagellum, for cases where the ratio (S/L) between the length of the flagellum and the wavelength of the bending waves is in the range of 1·2–1·5, as in the normal swimming patterns of sea-urchin and similar spermatozoa.

These results suggest that the rate of propagation of bending and unbending points cannot be determined independently by the resistance each point encounters as it propagates. In the simplest case the flagellum might be expected to produce the same active bending moment all along its length, and the propagation velocity might be expected to vary more or less inversely with the moment resisting bending or unbending. Examination of the records of bend propagation gives no indication of a correlation of this nature between the propagation velocity and the calculated bending moments. On the contrary, the propagation velocity is generally low in the region of low or negative bending moment near the base of the flagellum, where bends are being generated, and is occasionally lower as a bending point approaches the distal end of the flagellum. The propagation velocity typically has its maximum value, and remains relatively constant, near the middle of the flagellum, where the moments resisting bending and unbending are greatest.

There is some evidence that a bent region may be a unit, composed of a bending and unbending point which cannot propagate independently of one another (Goldstein, 1969). If the bent region is considered as a unit, the sum, $B+U$, of the resistances to bending and unbending at each end of the bent region may be the parameter which

might influence the propagation velocity. When S/L has values of 1·2–1·5, $B+U$ appears to remain relatively constant over most of the interval between the time the bend is fully developed and the time the bending point reaches the end of the flagellum. If the propagation velocity of a bend were regulated by the resistance $(B+U)$, no detectable variations in velocity could be predicted in these cases. However, for longer flagella, where S/L is about 1·75, the resistance $B+U$ is more sharply peaked. Photographs of flagellar movement with longer values of S/L have not been studied in detail, but no indications of irregularities in propagation velocity are obvious in such cases.

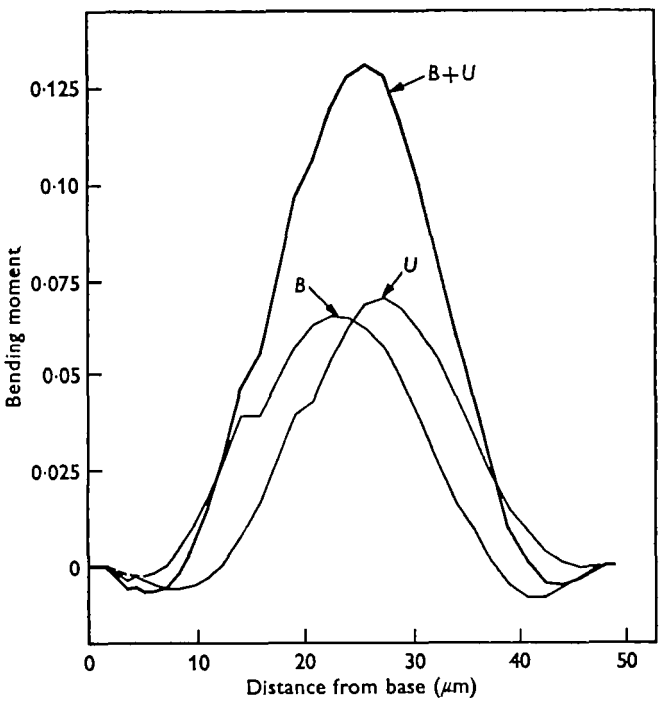

Text-fig. 10. The bending moment curves of Text-fig. 7A have been replotted to show the resisting moments at the bending and unbending points as a function of position on the flagellum instead of a function of time.

In Text-fig. 10 the bending moments from Text-fig. 7A have been replotted to show the variation in moment as a function of position along the flagellum. Although the peak moments for a bending point and the following unbending point are separated in time, as shown in Text-fig. 7A, they both occur near the middle of the flagellum. The sum $B+U$ in this case is an indication of the total amount of work done per beat cycle in propagating bending points, at each position along the flagellum. Points near the middle of the flagellum are required to work at about 2·5 times the average rate, while points near the distal end of the flagellum do no positive work at any time in the beat cycle. This last conclusion may be relevant to the presence of a thin terminal piece at the end of the sea-urchin sperm flagellum.

In previous discussion of the use of ATP dephosphorylation energy to perform the work required for flagellar bending, it was implicitly assumed that in flagella propa-

gating uniform bending waves the work done was distributed uniformly along the flagellum (Brokaw, 1968). A similar conclusion was reached by Rikmenspoel (1965). This is now seen to be untrue. In flagella, as in cilia (Sleigh & Holwill, 1969), different amounts of external work against viscous resistances are done by bending at various positions along the flagellum. Previous discussions of the energetics of flagellar movement have also indicated that the uniform use of 1 ATP molecule per beat by each flagellar ATPase molecule would provide 2–3 times the amount of energy needed for movement of the flagellum (depending on the value chosen for the free energy available from ATP dephosphorylation). The peak work performed per unit length in the mid-region of the flagellum is therefore just about equal to the absolute maximum amount of energy available, if energy is made available and used locally and if only one ATP molecule can be used at each ATPase site per beat cycle.

If the flagellum contains a conservative elastic resistance to bending, the bending moment resulting from elasticity will be proportional to the curvature of the flagellum if the flagellum behaves as a simple elastic structure obeying Hooke's law. This can be expressed as $M_e = \alpha/\rho$, where α is a constant representing the stiffness of the flagellum, and ρ is the radius of curvature at the point where the elastic bending moment, M_e, is measured. In the distal region of the flagellum, where ρ is approximately constant, the total moment resisting bending or unbending can be estimated by adding a constant value of M_e to the B curves and subtracting M_e from the U curves. The $B+U$ curves will be unchanged. The elastic moment within the flagellum represents work stored during bending, which may be available for use during unbending. If the value of α is sufficiently great, the total moment resisting unbending can always be negative, and no active work need be done by the flagellum at the unbending points. However, the system as a whole cannot operate conservatively unless some mechanism, such as a reconversion of stored elastic energy into chemical free energy, exists to utilize the 'negative work' of unbending when the moment resisting unbending is less than 0. If no such mechanism is present, the overall efficiency of the system will decrease as the stiffness of the flagellum is increased. In the case of the flagellum for which bending moments are shown in Text-fig. 7A, the value of stiffness which will be just sufficient to enable unbending to occur passively, utilizing only stored elastic work, is such that only about one-half of the total mechanical work done by the flagellum will appear as work done in moving against external viscous resistances; the remainder of the work is done against the elastic resistance to bending, but this energy stored in the elastic elements cannot be recovered as mechanical work against the viscous resistances. At higher values of stiffness the flagellum will become progressively less efficient, and its movements will probably become relatively insensitive to the viscosity of the medium.

Some objections raised previously (Gray, 1928; Brokaw, 1968) to the idea that unbending of a cilium or flagellum can be driven by stored elastic energy depend on the assumption that the rate of unbending in such cases would be determined by the elastic moment and the viscous moment resisting unbending. Since the results of this paper suggest that in general the propagation of bends along flagella must be controlled by a mechanism which is independent of local values of the bending moments, these objections become less forceful. The results of an earlier study of the effects of viscosity on sperm movement (Brokaw, 1966*b*) can be interpreted to mean that there is a

limit to the value of the viscous bending moment, which can be increased only in cases where the curvature of the flagellum increases. This behaviour is consistent with the possibility that unbending is a purely passive process, but a more thorough re-evaluation of the results of that study, using the methods for bending moment calculation developed in the present paper, would be desirable.

If each bent region is an integrated unit, rather than just the region between independently propagating bending and unbending points, the role of elastic resistances is difficult to evaluate without a more specific model. It is possible that within such a unit the elastic energy of bending and unbending could be conserved irrespective of the local values of the viscous bending resistances, so that the work done would be proportional to the $B+U$ curve in the distal part of the flagellum where bends are uniformly propagated. However, the elastic work done in initiating a bent region will probably not be recovered when this bent region reaches the distal end of the flagellum, so that a certain amount of non-conservative work against elastic resistances will be done during each beat cycle. A value for the stiffness constant, α, which will cause 50% of the total work output of the flagellum of Text-fig. 7A to be used non-conservatively against elastic bending resistances can be calculated for this case. This value of α will correspond to a bending moment in the bent regions which is 2·5 times the peak bending moment required to overcome viscous resistances, and will require that the rate of working during formation of a bent region near the base of the flagellum is 4–5 times the peak power output required to propagate a bend against viscous resistances. Further investigation of this model might be profitable.

Little can be said about other possible non-conservative bending resistances within the flagellum, except that they will reduce the efficiency of movement, especially at low external viscosities.

In discussing the results of his original examination of the bending waves of sea-urchin sperm flagella, Sir James Gray proposed a model in which independent, local, contractile elements were distributed along the sides of the flagellum (Gray, 1955). Other models of a similar nature can be imagined in which bending at a point depends on the independent activity, within the flagellum at that point, of some bend-generating mechanism, which may not necessarily involve contraction of elements at the sides of the flagellum. Electron microscopy suggests that these mechanisms are alike throughout the length of these flagella. It is then necessary to ask how the activity of these independent, bend-generating elements distributed along the flagellum might be controlled to produce various types of propagated bending waves.

Machin (1958, 1963) has discussed the possibility that bending-wave propagation is co-ordinated by visco-elastic interactions between the independent bending elements, in the same way that the elements of an elastic filament surrounded by a viscous medium interact in passively propagating waves driven by oscillation of one part of the filament. He suggests that passive bending of the flagellum, which will occur in regions where the sum of the elastic and viscous resistances to bending is negative, stimulates active bending. This mechanism has been objected to because it cannot easily explain the control of bending in cilia and in flagella propagating very asymmetical bending patterns (Brokaw, 1966*a*, 1968). The present results suggest that similar difficulties may be encountered in applying this mechanism to the uniform bending patterns of flagella. For uniform propagation this mechanism would appear to require

a constant time relationship between regions of negative bending resistance, where passive bending could initiate active bending, and the points where active bending occurs. However, the calculated bending-moment curves show that the moments are related more to the location along the flagellum and the length of the flagellum than to the phase of the bending.

An alternative mechanism for bend propagation was suggested by Brokaw (1966*a*), who pointed out that localized bending elements will probably not be completely independent, because of local shear strain near the bending and unbending points. This effect could provide a mechanism for a local point-to-point propagation of the activation of bending and unbending points, but overall co-ordination of the bending pattern would require a mechanism for controlling the propagation velocity. The calculations of bending moments indicate that this control of propagation velocity cannot be brought about by the bending moments resulting from viscous interactions between the bending of different parts of the flagellum.

It now appears unlikely that bent regions or their bending and unbending points reflect the activity of completely independent, local, bend-generating elements, which are co-ordinated solely by interaction through the mechanical properties of the viscoelastic system in which they are found. There must be some form of interaction within the flagellum, to provide for co-ordination between the activity of the bend-generating elements. Additional evidence suggesting such an interaction is provided by Goldstein's observation of an immediate decrease in propagation velocity of bends in the distal region of a flagellum when it was irradiated near its base by a laser beam (Goldstein, 1969).

The observation that in flagella, as well as in cilia, the work done by bending and unbending is not uniform along the length of the flagellum suggests that the use of chemical energy may also not be distributed uniformly along the flagellum. Alternatively, it may be better to discard the idea that the bending observed at one point on the flagellum is solely the result of active mechanochemical processes occurring in the interior of the flagellum at that point. For example, models in which bending is generated by sliding filaments, discussed by Satir (1967) and by Sleigh (1968), may provide a means for distributing the work required for bending at a particular point over a larger fraction of the length of the flagellum, and may also provide for interaction between different parts of the flagellum to co-ordinate the behaviour of the bending and unbending points. However, the details of a sliding filament model have not yet been sufficiently explored to allow comparison with experimental results.

SUMMARY

1. Starting with the simple hydrodynamic assumptions of earlier work on flagellar movement, an exact analysis of the bending moments in a flagellum moving through a viscous solution has been developed. The results illustrate the variation in the resistance to bending and unbending resulting from viscous forces as a function of time as bends move along a flagellum. These bending moments are 0 at free ends of the flagellum, and rise to peak values of 2–3 times their average value near the middle of the flagellum, for movement patterns similar to those normally found on sea-urchin spermatozoa.

2. The approximate expressions for bending moments and energy expenditures

developed in earlier work are reasonable estimates of the average values of these quantities.

3. Bending and unbending points propagate at reasonably constant velocities in the distal portion of free-swimming flagella, in spite of the large variations in the resisting moment resulting from viscous forces. The propagation velocity of individual bending and unbending points, or an individual bent region, is therefore probably not controlled by the resistance to bending and unbending at these points. Some mechanism for internal coordination of the activity of different regions of the flagellum appears to be required.

4. In flagella, as in cilia, the external work done against viscous resistances is not uniformly distributed along the length of the flagellum.

5. These conclusions provide additional support for 'sliding filament' models of flagellar bending.

REFERENCES

BROKAW, C. J. (1965). Non-sinusoidal bending waves of sperm flagella. *J. exp. Biol.* **43**, 155–69.

BROKAW, C. J. (1966*a*). Bend propagation along flagella. *Nature, Lond.* **209**, 161–3.

BROKAW, C. J. (1966*b*). Effects of increased viscosity on the movements of some invertebrate spermatozoa. *J. exp. Biol.* **45**, 113–39.

BROKAW, C. J. (1968). Mechanisms of sperm movement. *Symp. Soc. exp. Biol.* **22**, 101–16.

BROKAW, C. J. & WRIGHT, L. (1963). Bending waves of the posterior flagellum of *Ceratium*. *Science, N.Y.* **142**, 1169–70.

BURGERS, J. M. (1938). On the motion of small particles of elongated form, suspended in a viscous medium. In *Second Report of Viscosity and Plasticity, Kon. Ned. Akad., Verhand.* (*Eerste Sectie*) **16** (4), 113–84.

GOLDSTEIN, S. F. (1969). Irradiation of sperm tails by laser microbeam. *J. exp. Biol.* **51**, 431–44.

GRAY, J. (1928). *Ciliary Movement.* Cambridge University Press.

GRAY, J. (1955). The movement of sea-urchin spermatozoa. *J. exp. Biol.* **32**, 775–801.

GRAY, J. & HANCOCK, G. J. (1955). The propulsion of sea-urchin spermatozoa. *J. exp. Biol.* **32**, 802–14.

HANCOCK, G. J. (1953). The self-propulsion of microscopic organisms through liquids. *Proc. Roy. Soc. Lond.* A, **217**, 96–121.

MACHIN, K. E. (1958). Wave propagation along flagella. *J. exp. Biol.* **35**, 796–806.

MACHIN, K. E. (1963). The control and synchronization of flagellar movement. *Proc. Roy Soc. Lond.* B, **158**, 88–104.

RIKMENSPOEL, R. (1965). The tail movement of bull spermatozoa. Observations and model calculations. *Biophys. J.* **5**, 365–92.

RIKMENSPOEL, R. (1966). Elastic properties of the sea urchin sperm flagellum. *Biophys. J.* **6**, 471–9.

SLEIGH, M. A. (1968). Patterns of ciliary beating. *Symp. Soc. exp. Biol.* **22**, 131–50.

SLEIGH, M. A. & HOLWILL, M. E. J. (1969). Energetics of ciliary movement in *Sabellaria* and *Mytilus*. *J. exp. Biol.* **50**, 733–43.

SATIR, P. (1967). Morphological aspects of ciliary motility. *J. gen. Physiol.* **50**, (6–2; suppl.), 241–58.

APPENDIX. MATHEMATICAL METHODS

The method used to compute bending moments in a finite flagellum is an extension of a method introduced by Gray & Hancock (1955) for their calculation of the swimming velocity of sea-urchin spermatozoa. It was later applied to flagellar bending waves containing circular arcs and straight lines (Brokaw, 1965) and used to obtain a preliminary estimate of bending moment and energy expenditure. The method makes the fundamental assumption that the external force on any short element, ds, of the length of the flagellum, resulting from its movement through a viscous medium at a steady velocity, can be represented by:

$$dF_N = -C_N V_N ds \tag{1}$$

and

$$dF_L = -C_L V_L ds. \tag{2}$$

dF_N and dF_L are, respectively, the normal and tangential components of force acting on the element ds; V_N and V_L are the normal and tangential components of the velocity of the element ds; and the normal and tangential drag coefficients, C_N and C_L, are assumed to be constants which are independent of position along the flagellum. The use of these equations involves the assumptions that the velocity field around the element ds is independent of the bending of other parts of the flagellum and that the changes in V_N and V_L with time are slow enough to justify use of these steady-field equations. Burgers' discussion of transient effects (Burgers, 1938, p. 118) indicates that after a step change in velocity, the velocity field will assume nearly equilibrium values out to a distance of 5 μ from the flagellum within about 0·6 msec, or one-fiftieth of the cycle time for normal flagellar movement. Therefore the steady-field assumption appears to be no worse than the assumption that the bending of distant parts of the flagellum does not influence the velocity field around a particular element ds. The most important error involved in these assumptions may be the assumption that the values of C_N and C_L remain the same near the end of a flagellum.

Although equations (1) and (2) represent a greatly oversimplified approach to the hydrodynamics of flagellar movement, previous work has shown that this approach leads to reasonably accurate estimates for the forward swimming velocity of spermatozoa and flagella, so that it appears at least to be valid as a first-order approximation.

The external forces acting on various elements of the flagellum will set up shearing forces and bending moments within the flagellum. Considering the flagellum as a very thin filament, these internal forces can be represented simply as functions of position along the length of the flagellum, and are given by the following equations:

$$F_N(s) = F_N(0) + \int_{s=0}^{s=s} dF_N \tag{3}$$

and

$$M(s) = M(0) + \int_0^s F_N\, ds. \tag{4}$$

F_N is the normal component of shear force within the flagellum and M is the bending moment. In previous work (Brokaw, 1965), $M(s)$ was obtained from these equations by arguing that in a long flagellum propagating symmetrical, uniform, bending waves, $M(s)$ would be zero at the crests of the bending waves and $F_N(s)$ would be zero at the points where the flagellum crossed the axis of symmetry of the wave. The values of M obtained in this way were constant for a particular phase point in the bending wave cycle. This approach ignored the fact that in any real flagellum, both $M(s)$ and $F_N(s)$ must be zero at a free end of the flagellum, regardless of the phase of the wave. The moment at a particular phase point (such as a bending or unbending point) must therefore decrease to zero as these points near the end of a flagellum, and cannot have the constant values given by the previous treatment at all points on the flagellum.

If V_N is known for all values of s along the flagellum, $M(s)$ can be evaluated accurately from equations (1), (3) and (4), by carrying out the integrations from a free end of the flagellum, where $M(s)$ and $F_N(s)$ must both be zero. In principle, V_N values could be obtained from measurements on a series of photographs of a flagellum taken at closely spaced time intervals ($<$ 0·1 beat period). This procedure is difficult, and probably not very accurate. Alternatively, if there is a consistent pattern of flagellar

bending which can be deduced from photographs of moving flagella and expressed in mathematical terms, V_N values can be calculated. This procedure was used in the previous studies by Gray & Hancock (1955) and by Brokaw (1965). In both cases, only symmetrical flagellar bending waves were considered, and rotation and lateral displacement of the flagellum were neglected. V_L and V_N were expressed as functions of the bending wave parameters and an unknown forward velocity. The component of force in the direction of the wave axis was integrated, starting from a free end where the force must be zero. Since there must also be zero force at the other free end of the flagellum, the value of this force integral can be set equal to zero, and the resulting expression can be solved to obtain a unique value for the forward velocity. Values of V_N and V_L could then be calculated and used to obtain values for the bending moment.

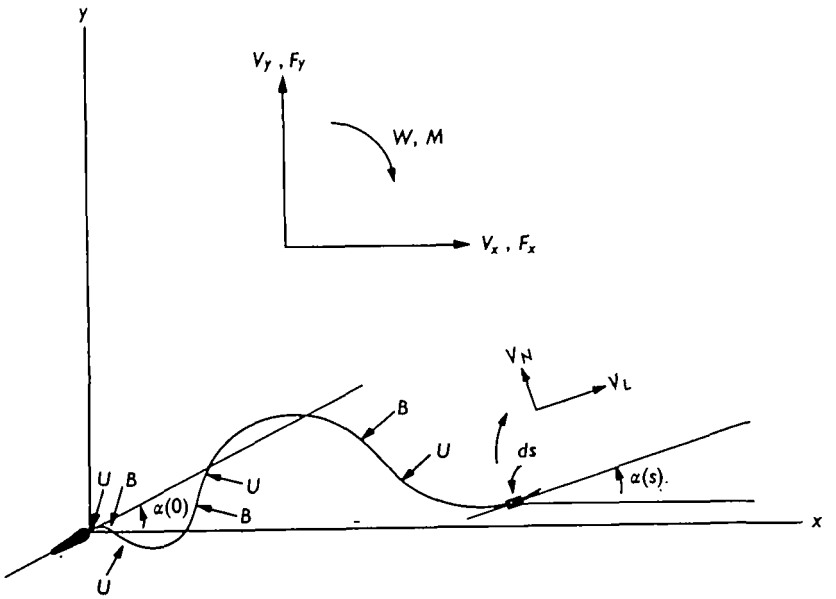

Text-fig. 11. Identification of some of the variables used in the computation of bending moments for the movement of a flagellum. Bending and unbending points are identified by *B* and *U*, respectively.

The availability of a computer for numerical integration of these procedures has now made it possible to carry out a more exact analysis incorporating the following improvements over earlier analyses.

Not only the forward velocity, but also the rotational and lateral velocities have been calculated, by integrating two force components and the bending moment over the flagellum and setting the integrals equal to zero at the free end of the flagellum. This makes it possible to deal with asymmetrical bending wave patterns, which normally cause swimming in a circular path.

The use of numerical integration makes it feasible to deal with mathematically more complex bending waves and to consider, in particular, a more detailed description of the bending in the basal region of the flagellum, where bends are initiated.

Realistic boundary conditions at the ends of the flagellum have been used. In order

to compute the moment at a particular phase point, such as a bending point, as a function of time or position on the flagellum, it is then necessary to carry out a complete calculation of bending moments for many times during a beat cycle. Use of the computer makes this feasible.

The mathematical analysis on which these computations were based is described in the following paragraphs.

The variables used for calculation are defined with reference to an x,y coordinate system having its origin at the anterior end of the sperm flagellum, as shown in Text-fig. 11. Only movements in the x,y plane are considered. $\alpha(s)$ is the angle between the tangent to the flagellum at any point s and the x axis; s is distance measured along the flagellum from the origin of the coordinate system. The forces and moment at any point s are then given by the following three equations;

$$F_x = -CH_x V_x - \sum_{i=1}^{4} \int_0^s (V_L(i)\, C_L \cos\alpha\, ds - V_N(i)\, C_N \sin\alpha\, ds), \tag{5}$$

$$F_y = -CH_y V_y - \sum_{1}^{4} \int_0^s (V_N(i)\, C_N \cos\alpha\, ds + V_L(i)\, C_L \sin\alpha\, ds), \tag{6}$$

$$M(s) = -CH_w W + \sum_{1}^{4} \int_0^s (F_y(i) \cos\alpha - F_x(i) \sin\alpha)\, ds. \tag{7}$$

F_x is the x component of the shear force within the flagellum at the point s; and F_y is the corresponding y component. V_x is the velocity of the co-ordinate system in the x direction; V_y is the velocity of the co-ordinate system in the y direction; and W is the angular velocity of the co-ordinate system, as defined in Text-fig. 11. CH_x, CH_y, and CH_w are drag coefficients for movement of the head of the spermatozoon. The index (i) refers to components of V_L, V_N, F_x, and F_y which result from four movements.

$i = 4$ refers to movement of points on the flagellum in the y direction resulting from overall movement of the flagellum and its coordinate system with the velocity V_y:

$$V_L(4) = V_y \sin\alpha, \tag{8}$$

$$V_N(4) = V_y \cos\alpha. \tag{9}$$

$i = 3$ refers to movement in the x direction resulting from the velocity V_x:

$$V_L(3) = V_x \cos\alpha, \tag{10}$$

$$V_L(3) = V_x \sin\alpha. \tag{11}$$

$i = 2$ refers to rotational movement resulting from the angular velocity W:

$$V_L(2) = W(y \cos\alpha - x \sin\alpha), \tag{12}$$

$$V_N(2) = W(-x \cos\alpha - y \sin\alpha); \tag{13}$$

where the x and y co-ordinates of a point s are obtained from the following integrals:

$$x = \int_0^s \cos\alpha\, ds, \tag{14}$$

and

$$y = \int_0^s \sin\alpha\, ds. \tag{15}$$

$i = 1$ refers to movement of a point s relative to the x,y co-ordinate system originating at the head end of the flagellum. This movement results from flagellar bending and unbending.

$$V_L(1) = \dot{x}\cos\alpha + \dot{y}\sin\alpha, \tag{16}$$

$$V_N(1) = \dot{y}\cos\alpha - \dot{x}\sin\alpha, \tag{17}$$

where

$$\dot{x} = -\int_0^s \sin\alpha\,(d\alpha/dt)\,ds, \tag{18}$$

$$\dot{y} = \int_0^s \cos\alpha\,(d\alpha/dt)\,ds \tag{19}$$

are obtained by differentiation of equations (14) and (15) with respect to time. If the wave is specified by giving α and $d\alpha/dt$ as functions of s, all the components can be integrated. At the distal end of the flagellum, the integrals giving F_x, F_y, and $M(s)$ must each equal 0, if this is a free end on which no external forces are acting. This produces three equations which can be solved for V_x, V_y, and W. These values of V_x, V_y and W can then be used to obtain values for $M(s)$ from equation (7). The entire procedure must be repeated, using appropriate specifications of α and $d\alpha/dt$, for other points in time through one cycle of flagellar bending, in order to obtain a complete picture of $M(s,t)$.

It is convenient to specify flagellar waves in terms of regions of constant curvature, separated by straight regions. This specification can be used to fit the flagellar photographs considered in this paper. The information required to obtain α and $d\alpha/dt$ as functions of s needs to be specified only at the points where the curvature changes, indicated by U or B in Text-fig. 11. At each of the bending and unbending points indicated in Text-fig. 11, let the following parameters be specified;

s = location of the bending or unbending point, measured along the flagellum from the head end,

$\Delta k(s)$ = change in curvature of the flagellum at point s,

$\Delta\dot{k}(s)$ = change in the time derivative of curvature at point s,

$V_s(s)$ = propagation velocity of the transition point.

$\Delta k(s)$ and $\Delta\dot{k}(s) = 0$ at all other points. α and $d\alpha/dt$ can be generated by equations (20)–(23):

$$\alpha = \alpha(0) + \int_0^s k(s)\,ds, \tag{20}$$

where

$$k(s) = \int_0^s \Delta k(s)\,ds. \tag{21}$$

The convention that $k(0) = 0$ at $s = 0$ has been adopted.

$$d\alpha/dt = \int_0^s dk(s)/dt\,ds, \tag{22}$$

where

$$dk(s)/dt = \int_0^s \Delta\dot{k}(s)\,ds - V_s(s)\Delta k(s). \tag{23}$$

The above method for calculating $M(s)$ is easily adapted to numerical integration on a digital computer. I have used a FORTRAN IV program involving simple trapezoidal integration, which starts at the head end of the flagellum and carries out all the integrations (equations 5–7, 14, 15, 18–23) simultaneously as it proceeds in steps along the flagellum. A value for the rate of working of the flagellum is also obtained by integrating $M(s)\,[dk(s)/dt]$ over the length of the flagellum. On Caltech's IBM 360/75 system, slightly less than 1 sec is required to compute bending moments for one position of a flagellum, using 1200 integration steps. Inspection of the symmetry of the results obtained for symmetrical waves indicates that errors are less than 0·5 % with this number of steps.

Computation can be carried out by supplying sets of parameters (s, $\Delta k(s)$, $\Delta\dot{k}(s)$, $V_s(s)$) for each of a number of times in the cycle of flagellar bending, or the program can be augmented so that these sets are generated automatically from more general information about the behaviour of the flagellum, such as the behaviour of V_s and the total angles of the bent regions as functions of time. It is also convenient to set up the program to collate bending moments for particular bending and unbending points and draw curves such as those in Text-figs. 6–9.

EXPLANATION OF PLATE

Fig. 1. Flagellum from a spermatozoon of *L. pictus*, photographed with ten evenly spaced flashes. This flagellum is running out of ATP. It has slowed down to less than 10 beats/sec and the dimensions of its bending waves have become larger than normal. The head end of the flagellum is towards the left side of the photograph.

Fig. 2. Flagellum from a spermatozoon of *L. pictus*, photographed with flashes at a frequency slightly slower than the frequency of beat. This flagellum was photographed more promptly after removal of the head; the parameters of its movement are close to those of flagella of normal spermatozoa. The flagellum is swimming in a clockwise circle.

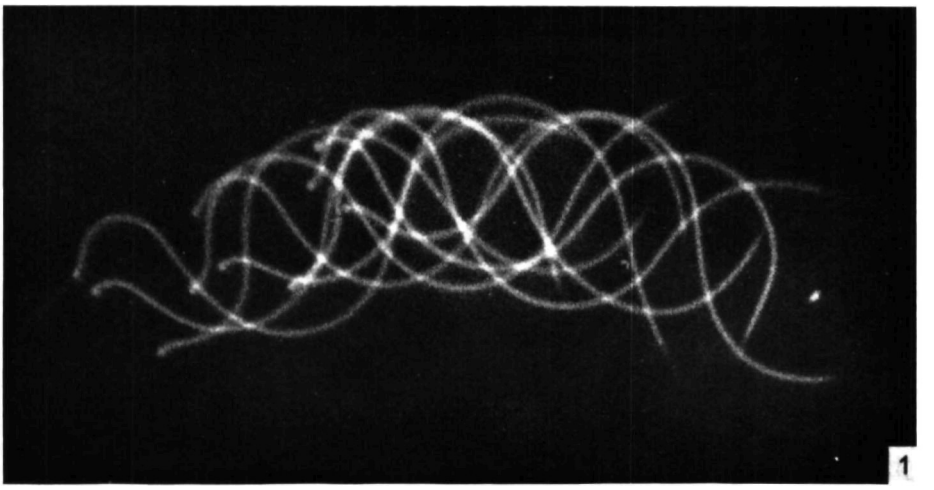
1

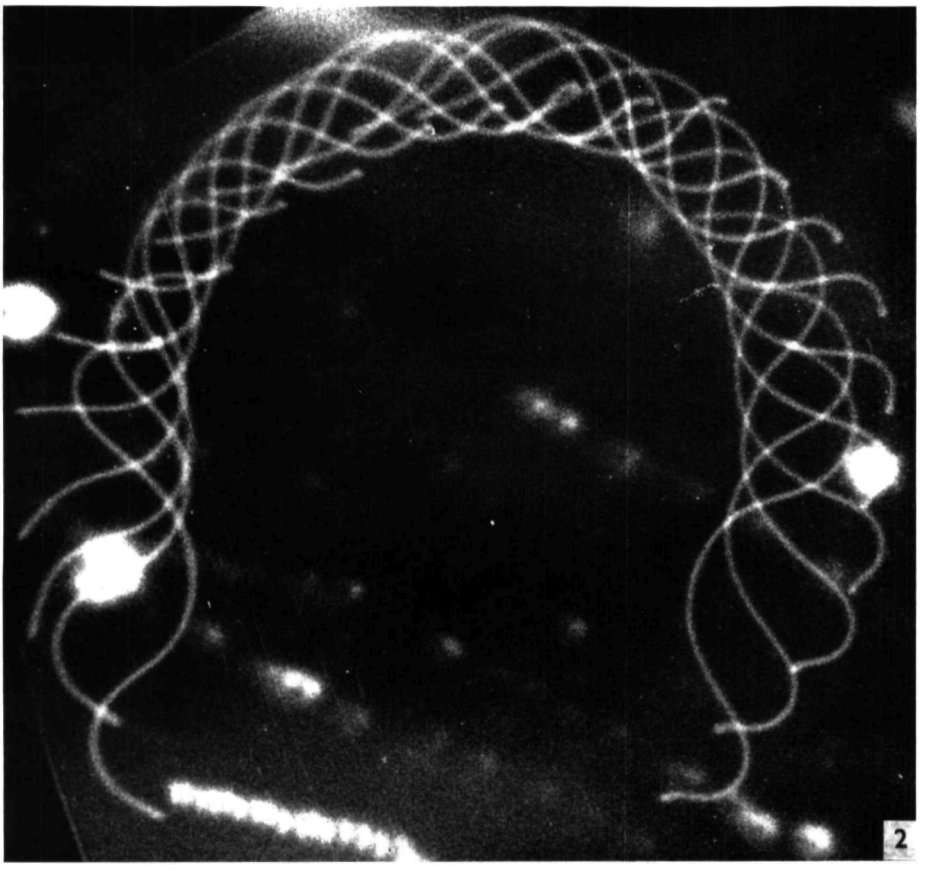
2
25 μm